

Supplementary material

Supplementary figures A1–A6.

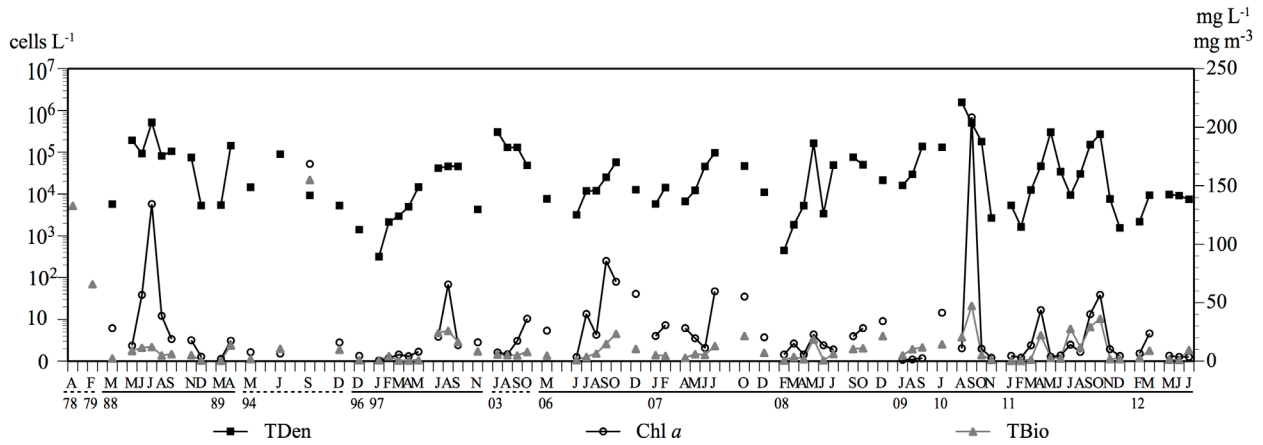


Fig. A1. Seasonal trends of TBio and Chl-*a* (in the first axis) and TDen (in the second axis) along the multiannual period.

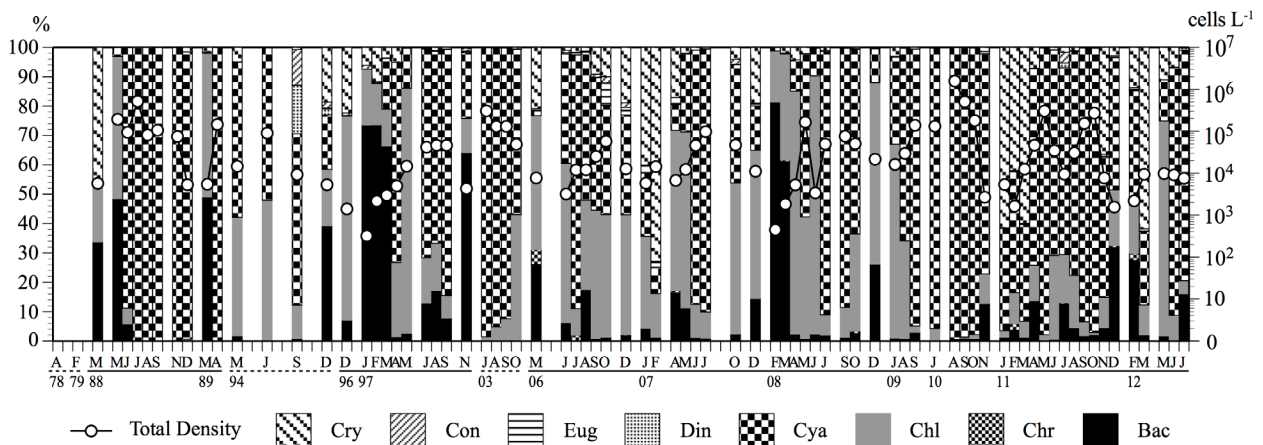


Fig. A2. Class composition of phytoplankton abundance (as column, in the first axis) and TDen values (as line, in the second axis) in the multiannual period (Cry = Cryptophyceae; Con = Conjugatophyceae; Eug = Euglenophyceae; Din = Dinophyceae; Cya = Cyanophyceae; Chl = Chlorophyceae; Chr = Chrysophyceae; Bac = Bacillariophyceae).

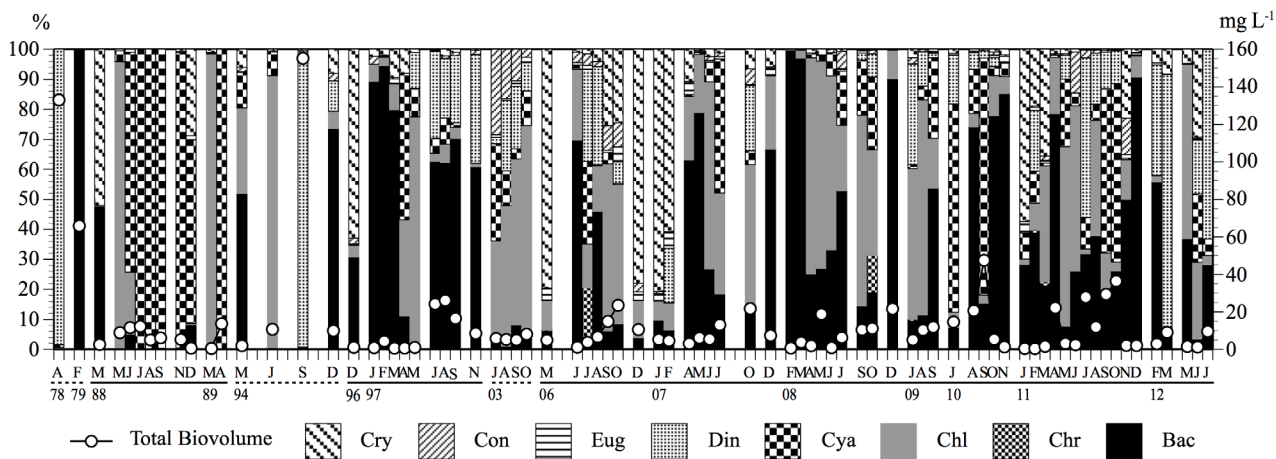


Fig. A3. Class composition of phytoplankton biomass (as column, in the first axis) and TBio values (as line, in the second axis) in the multiannual period (Cry = Cryptophyceae; Con = Conjugatophyceae; Eug = Euglenophyceae; Din = Dinophyceae; Cya = Cyanophyceae; Chl = Chlorophyceae; Chr = Chrysophyceae; Bac = Bacillariophyceae).

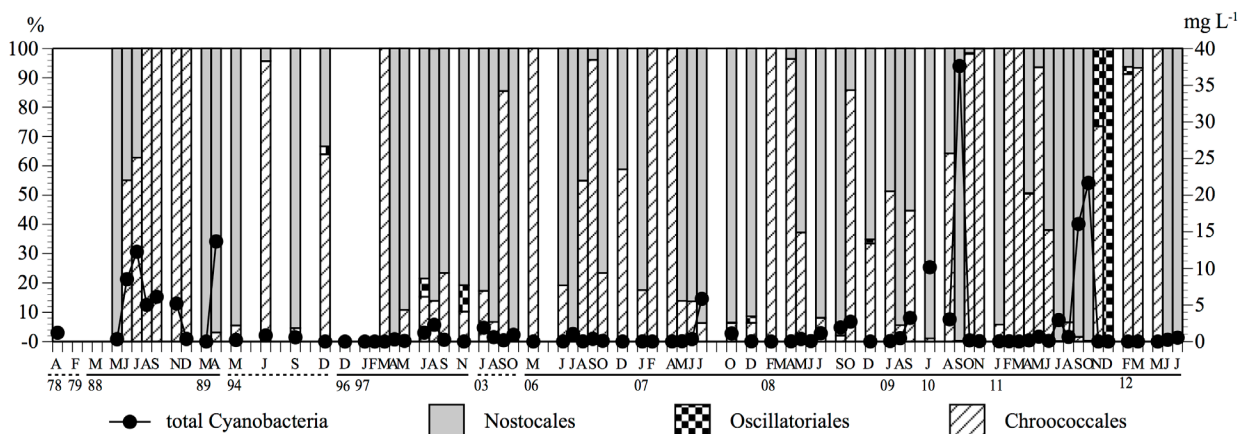


Fig. A4. Orders composition of Cyanobacteria (as column, in the first axis) and total Cyanobacteria biomass (as line, in the second axis) in the multiannual period.

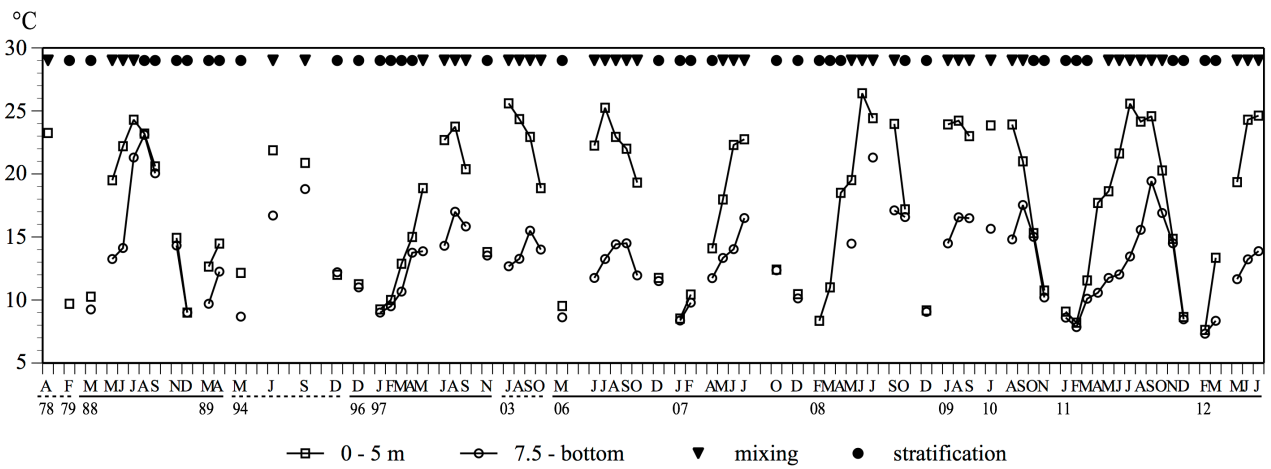


Fig. A5. Multiannual seasonal variation in the water temperature as mean values in the epilimnion (0–5 m) and ipolimnion (7.5 m–bottom). Stratification phase ▼; mixing phase ●.

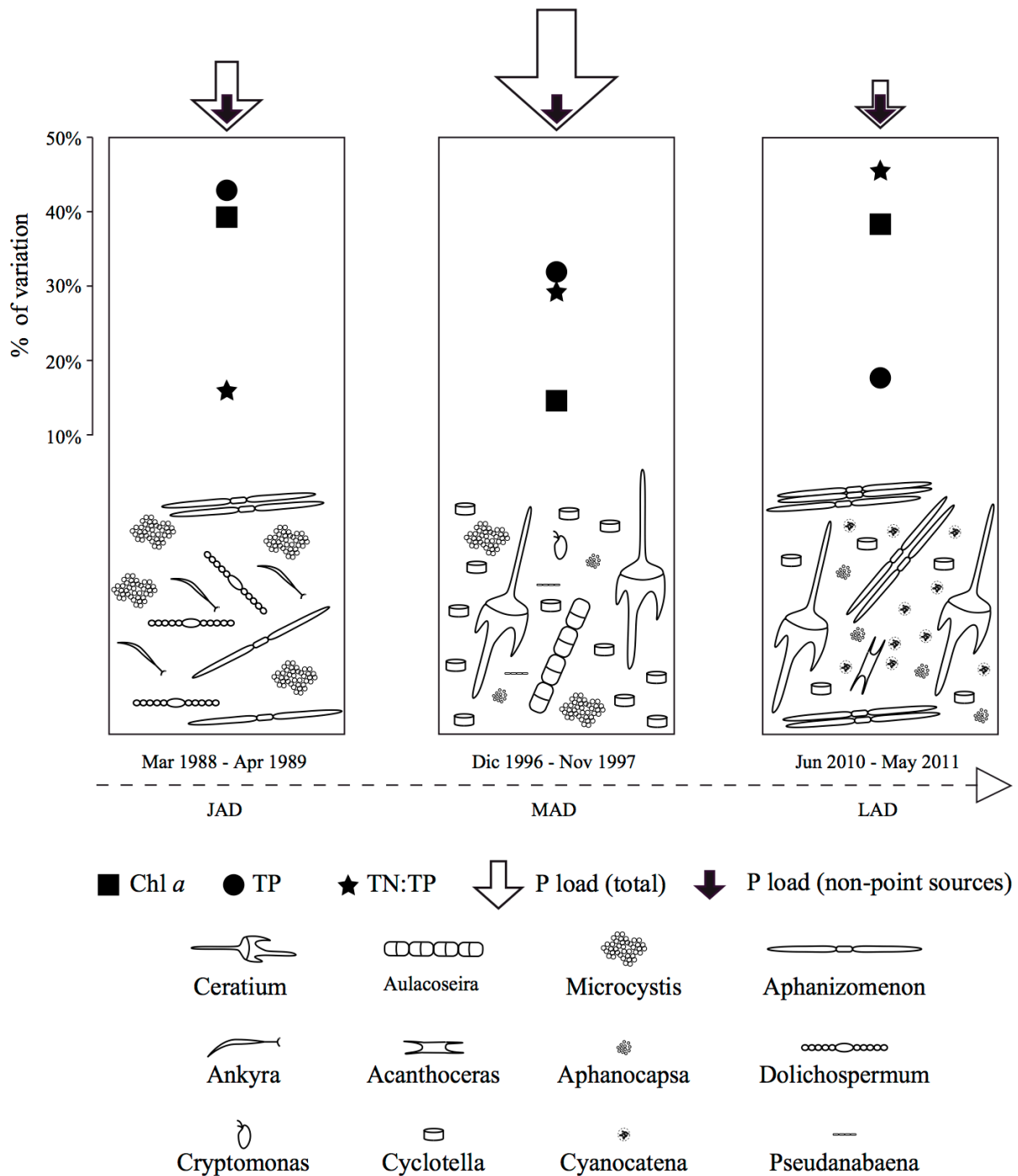


Fig. A6. Conceptual model of the main phytoplankton species succession that affected Bidighinzu Lake during JAD (just after diversion, 1988–1989), MAD (mid-diversion, 1994–1997), and LAD (long after diversion, 16–22 years). The percentage of variations of Chl-*a*, TP, and TN:TP were reported in the axis on the left.